Gamma Ray Spectroscopy With a $\varnothing 19 \times 19\ \mathrm{mm}^3\ LaBr_3 : 0.5\%\ Ce^{3+}$ Scintillator

P. Dorenbos, J. T. M. de Haas, and C. W. E. van Eijk, *Member, IEEE*

***Abstract*—Pulse height spectra of various sources covering X-ray and gamma ray energies from 10 keV to 6.1 MeV were measured by the first large $\varnothing 19 \times 19\ \mathrm{mm}^3\ LaBr_3 : 0.5\%\ Ce^{3+}$ scintillator. The spectra are compared with that recorded with a same sized NaI:Tl^+ scintillator. Excellent energy resolution pulse height spectra are obtained showing that the scaling up from a small ($\approx 3 \times 3 \times 10\ \mathrm{mm}^3$) sized $LaBr_3 : Ce^{3+}$ scintillator studied initially up to an $\approx 6\ \mathrm{cm}^3$ scintillator does not lead to much deterioration of resolution and light output. Special attention is devoted to the nonproportionality in the response of $LaBr_3 : Ce^{3+}$ and related energy resolution. At high energy $LaBr_3 : Ce^{3+}$ is far superior above NaI:Tl^+ in terms of energy resolution and scintillation speed. At energies below 100 keV, NaI:Tl^+ shows a better energy resolution.**

***Index Terms*—Energy resolution, gamma ray spectroscopy, $LaBr_3 : Ce^{3+}$, nonproportionality, scintillator.**

I. Introduction

In 2001, we introduced the new scintillator $LaBr_3 : Ce^{3+}$. Crystals with typical sizes of $3 \times 3 \times 10\ \mathrm{mm}^3$ and Ce^{3+} concentrations varying from 0.5 to 10% were studied [1]–[3]. A light yield of 61 000 photons per MeV of absorbed gamma ray energy (ph/MeV), energy resolution of $\approx 3\%$ (FWHM) at 662 keV, combined with a decay time of 35 ns and no intense slow components and afterglow make $LaBr_3 : 0.5\%Ce^{3+}$ superior to the most widely used scintillator NaI:Tl^+. The density is 5.3 $\mathrm{g/cm}^3$. Increasing the Ce^{3+} concentration above 2% results in even faster decay of 15 ns.

The properties of $LaBr_3 : Ce^{3+}$, and also of $LaCl_3 : Ce^{3+}$ discovered one year earlier[4], make these scintillators promising for many different applications. High resolution gamma ray spectroscopy is one of them [5], and especially the fast decay of 15 ns allows combining this with fast timing applications [6]. $LaBr_3 : Ce^{3+}$ is seriously considered as scintillator in positron emission tomography (PET) applications [7], [8]. A timing resolution as short as 250 ps was demonstrated which makes $LaBr_3 : Ce^{3+}$ interesting for time of flight PET [6], [8] and a first prototype 10×10 multicrystal array already demonstrated the properties for PET applications [8].

Within three years after our initial report, the growth of $LaBr_3 : Ce$ has been scaled up to sizes of $\varnothing 19 \times 19\ \mathrm{mm}^3$. The material is hygroscopic and needs to be contained in a sealed casing with appropriate reflecting covering. The technology has been developed, and in this work we present results on the first prototype scintillator. The very good scintillation properties, which were observed initially on small laboratory sized samples, are maintained on the large crystal. To demonstrate the properties, pulse height spectra of a variety of gamma ray sources are presented covering energies from 10 keV to 6.1 MeV. They are compared with the spectra recorded under identical circumstances with an equal sized NaI:Tl scintillator. From the spectra the energy resolution and the proportionality in the scintillation light output as function of gamma ray energy are determined.

II. Experimental

The $LaBr_3$ scintillator doped with 0.5% Ce^{3+} was grown by the vertical Bridgman technique by the crystals and detectors division of Saint Gobain, Nemours, France. The $\varnothing 19 \times 19\ \mathrm{mm}^3$ crystal was cut and polished from a larger size crystal boule. The crystal is surrounded with reflecting material and encased in a metal container that is hermetically sealed off with a glass window. A NaI:Tl crystal of the same dimensions and from the same manufacturer was used for comparison.

The scintillators are mounted on the quartz window of a Hamamatsu R1791 photomultiplier tube (PMT). A grease (General Electric Viscasil 60 000 cSt) was used for optical coupling between the scintillator and the window of the PMT. An Amersham variable X-ray source was used to excite the crystals at energies between 13.4 and 44.5 keV. ^{241}Am produces characteristic K_α and K_β X-rays from Rb, Mo, Ag, Ba, and Tb targets. ^{241}Am, ^{133}Ba, ^{137}Cs, ^{22}Na, and ^{60}Co gamma rays sources were used for exciting with gamma ray energies between 59.5 keV and 1.33 MeV. High energy gamma rays of 1.37 MeV and 2.75 MeV are emitted by a ^{24}Na source obtained by neutron activation in the reactor at our institute. A $^{238}Pu(^{13}C)$ source produces 6129 keV gamma rays by the reaction $^{13}C(\alpha, n\gamma)^{16}O$, where the α particles are produced by the decay of ^{238}Pu.

The PMT with scintillator is in a light tight aluminum housing. Pulse height spectra were recorded with the source outside the housing and positioned along the cylindrical axis of the scintillator about 3–5 cm above its top face. After pre-amplification the pulses were shaped by a spectroscopy amplifier. A shaping time of 0.5 μs was used with the $LaBr_3 : Ce^{3+}$ scintillator and 3.0 μs was used with NaI:Tl^+. By removing the source and increasing the amplifier gain, the single photo-electron pulse height spectrum was recorded. With these spectra, the gamma ray spectra were calibrated in terms of the number of photoelectrons created per MeV of absorbed gamma ray energy [9].

Manuscript received January 19, 2004; revised February 13, 2004. This work was supported by the Dutch Technology Foundation (STW) and the United States Department of Energy.

The authors are with the Interfaculty Reactor Institute, Delft University of Technology, 2629JB Delft, The Netherlands (e-mail: dorenbos@iri.tudelft.nl).

Digital Object Identifier 10.1109/TNS.2004.829375

0018-9499/04$20.00 © 2004 IEEE

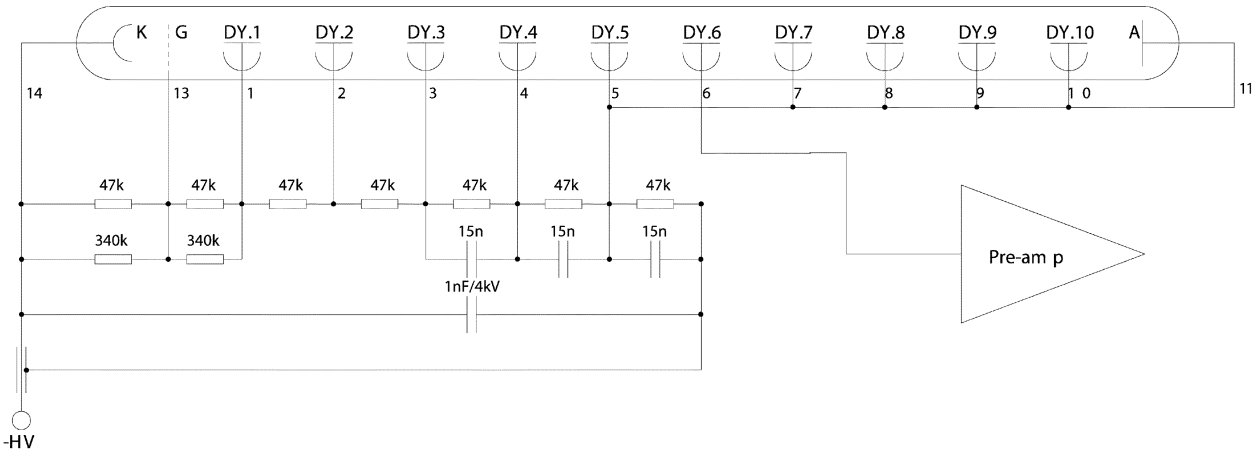

Fig. 1. Electronic scheme of the voltage divider.

Because of the high light yield of $LaBr_3:Ce^{3+}$ combined with a very fast decay, the peak currents flowing through the photomultiplier tube are more than ten times larger than when NaI:Tl is used. Especially when high gamma ray energies (1–6 MeV) are involved this may lead to nonlinearity in the PMT gain and a distorted pulse height spectrum results. The Hamamatsu R1791 PMT is a 10 dynode stage box and grid type PMT with bi-alkali photocathode. To cope with high peak currents we used a voltage divider scheme as shown in Fig. 1. The signal is obtained from the sixth dynode at ground potential. The anode and dynodes 7–10 are at the same potential as dynode 5 in order to obtain a good charge collection on dynode 6. The photocathode is at V_c Volt.

Fig. 2 shows ^{60}Co pulse height spectra measured at $V_c = -700$ V and $V_c = -500$ V. Both spectra where scaled to coincide at energies around 300 keV. At $V_c = -700$ V, a clear nonlinearity is evidenced in the high energy region where the 1.17 and 1.33 MeV total absorption peaks are shifted toward smaller pulse heights. In the experiments, we carefully avoided PMT gain nonlinearity by selecting a proper cathode voltage.

Decay time spectra were recorded by a conventional single photon start-stop method using a ^{22}Na source emitting two coincident 511 keV gamma rays. One gamma ray is detected in a BaF_2 scintillator and creates the start signal. The other gamma ray is detected in the canned $LaBr_3:Ce^{3+}$ scintillator and creates the stop signal. Two fast linear focused XP2020Q PMTs were used [9].

III. Results and Discussion

This section is divided into several subsections. First, some general aspects of $LaBr_3:Ce^{3+}$ and $NaI:Tl^+$ are presented like the linear attenuation coefficients for photo-electric absorption, Compton scattering, and pair creation. This information together with energies and probabilities of K_α and K_β X-ray fluorescence is needed to interpret the pulse height spectra. By analyzing the ^{24}Na gamma ray pulse height spectrum measured with $LaBr_3:Ce^{3+}$ features like, total absorption peak, Compton edge, 511 keV escape peak, backscatter peak are illustrated. Next gamma ray pulse height spectra measured with $LaBr_3:Ce^{3+}$ are compared with those measured with

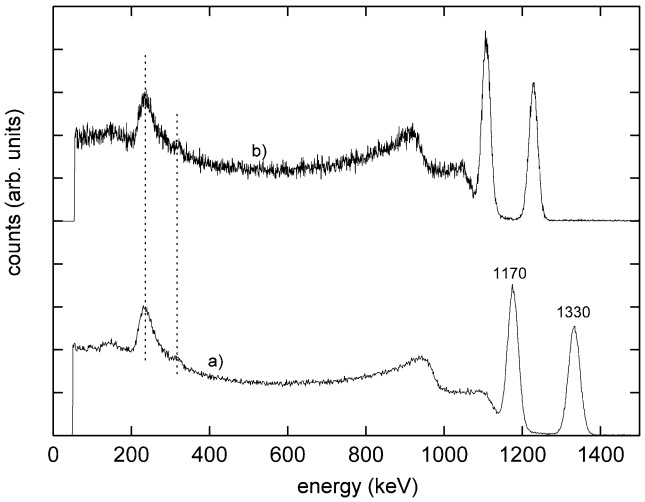

Fig. 2. ^{60}Co gamma ray pulse height spectra measured with $LaBr_3:Ce^{3+}$ at cathode voltages a) $V_c = -500$ V and b) $V_c = -700$ V.

$NaI:Tl^+$. The much better performance of $LaBr_3:Ce^{3+}$ regarding energy resolution and linearity is demonstrated. Further analysis of the pulse height spectra provides information on the photoelectron yield/MeV and the nonlinearity with gamma ray energy. Finally, aspects of energy resolution are presented.

A. General Aspects

Fig. 3 shows the photoelectric absorption, Compton scattering, and pair creation linear attenuation coefficients calculated for $LaBr_3$ ($\rho = 5.3$ g/cm^3) and NaI ($\rho = 3.7$ g/cm^3). For energies between 40 keV and 10 MeV the photoelectric absorption coefficients are almost identical. $LaBr_3$ shows 40% larger Compton scattering coefficient, and also the pair creation coefficient at energies larger than 3 MeV is $\approx 25\%$ larger than for NaI.

Fig. 4 shows the decay time spectrum of the scintillation pulse from $LaBr_3:0.5\%\ Ce^{3+}$. The pulse reveals a rise time before the exponential decay with a decay time $\tau = 30.2$ ns sets in. Apparently, there is a delay in the excitation of Ce^{3+} that has to do with the transport of charge carriers from the host to the Ce^{3+} centers. The value of 30.2 ns is 5 ns shorter than reported before on the $3 \times 3 \times 10$ mm^3 sample [2]. This is probably due to

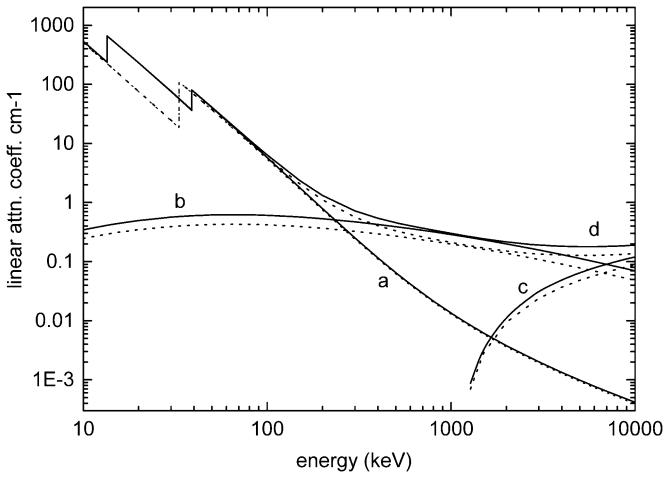

Fig. 3. Linear attenuation coefficients for (solid curves) $LaBr_3$ and (dashed curves) NaI: a) photoelectric absorption; b) compton scattering; c) pair creation; d) total.

a slightly higher Ce^{3+} concentration. When the Ce^{3+} concentration is above 2%, the decay time becomes shorter. The decay spectrum b) was measured for a small $3 \times 3 \times 8\ \mathrm{mm}^3$ $LaBr_3$ crystals with 4% Ce^{3+}. It shows a shorter rise time with a fast exponential decay of 15 ns. For comparison also the decay spectrum of NaI:Tl^+ is shown, see spectrum c). With a decay time of 230 ns it is 15 times slower than $LaBr_3:4\%Ce^{3+}$.

B. The Anatomy of Pulse Height Spectra

Fig. 5 shows the gamma ray pulse height spectrum of the ^{24}Na source measured with the large $LaBr_3:Ce^{3+}$ crystal at $V_c = -300$ V. Assuming a linear response with gamma ray energy, that actually appears to be the case quite well for $LaBr_3:Ce^{3+}$, a linear energy scale can be used. The spectrum is very rich in features that are, in order of decreasing energy, numbered 1 to 15. Starting on the high energy side we first observe the total absorption peak (1) at 2.75 MeV caused by: a) photoelectric absorption ($\mu_{pe} = 0.0023\ \mathrm{cm}^{-1}$); b) Compton scattering ($\mu_C = 0.165\ \mathrm{cm}^{-1}$) followed by photoelectric absorption of the scattered gamma ray; and c) pair creation ($\mu_{pc} = 0.026\ \mathrm{cm}^{-1}$) followed by absorption of 511 keV annihilation quanta. The maximum energy $E_C(E_\gamma)$ transferred to the electron in Compton scattering is

$$E_C(E_\gamma) = \frac{2E_\gamma^2}{511 + 2E_\gamma} \tag{1}$$

and it gives the Compton edge at $E_C(2750) = 2520\,\mathrm{keV}$ which is denoted by feature (3) in Fig. 5. When a gamma ray undergoes multiple Compton scattering interaction in the scintillator it contributes to the counts in the tail at (2).

A part of the 2.75 MeV gamma rays is absorbed by pair creation. The positron looses its kinetic energy and subsequently annihilates with an electron creating two 511 keV gamma rays that may or may not escape from the crystal. Assuming the same escape probability p for both collinearly emitted 511 keV gamma quanta, the probabilities for zero single and double 511 keV escape are given by $P(0) = 1 - 2p + p^2$, $P(1) = 2p(1-p)$ and $P(2) = p^2$. Features (7) and (5) at 1732 keV and 2243 keV are the double and single 511 keV escape peaks. From the ratio of intensities, we estimate an

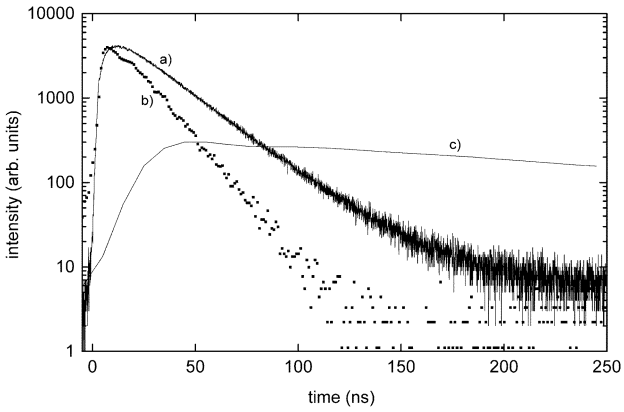

Fig. 4. Gamma ray excited scintillation decay time spectra of: a) the $\varnothing 19 \times 19\,\mathrm{mm}^3$ $LaBr_3:0.5\%Ce^{3+}$; b) a small $3 \times 3 \times 8\ \mathrm{mm}^3$ $LaBr_3:4\%Ce^{3+}$ sample; and c) NaI:Tl^+.

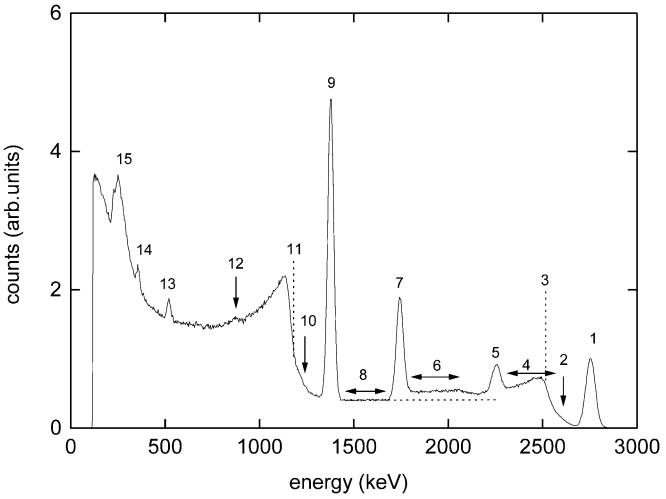

Fig. 5. The ^{24}Na gamma ray pulse height spectrum measured with $LaBr_3:Ce^{3+}$. Features 1 to 15 are discussed in the text. The horizontal dashed line indicates the compton background from 2.754 MeV gamma rays. Dashed vertical lines indicate the location of compton edges.

escape probability of $p = 0.88$. Then $P(0)$ is more than 50 times smaller than $P(2)$. This and the attenuation coefficients demonstrate that the dominant contribution to peak (1) is from Compton scattering followed by photoelectric absorption of the scattered gamma ray.

511 keV annihilation quanta Compton scattered in the scintillator with escape of the scattered gamma ray lead to features (6) and (4) on top of the Compton background from 2.75 MeV gamma rays. These features extend to 2073 keV, i.e., 170 keV below the single 511 keV escape peak (5), and to 2584 keV, i.e., 170 keV below the total absorption peak (1).

The pulse height spectrum is flat between 1450 keV and 1650 keV (8). This is the only part of the spectrum that is composed of one single contribution, i.e., from Compton scattering of 2.75 MeV gamma rays only. Peak (9) is the total absorption peak of 1.37 MeV gamma rays. Pair creation leads to the faint double (14) and single (12) 511 keV escape peaks with (almost) the same escape probability and intensity ratios as for escape peaks (7) and (5).

The Compton edge (11) starts below $E_C(1380) = 1160\,\mathrm{keV}$ with a tail (10) due to multiple Compton scattering. Absorption

of 1.37 and 2.75 MeV gamma rays outside the scintillator either by pair creation or Compton scattering and subsequent detection of 511 keV annihilation gamma ray or the Compton scattered gamma ray leads to the 511 keV back scatter peak (13) and the Compton back scatter events (15) at around 250 keV.

C. $LaBr_3$:Ce^{3+} and NaI:Tl^+ Pulse Height Spectra

In the following, we compare the gamma ray pulse height spectrum measured with the $\varnothing 19 \times 19\,\mathrm{mm}^3$ $\mathrm{LaBr_3:Ce^{3+}}$ with that measured under identical circumstances (apart occasionally from the cathode voltage) with the $\varnothing 19 \times 19\ \mathrm{mm}^3$ NaI:Tl^+ scintillator. In presenting the spectra we will assume a linear relationship between pulse height and detected amount of ionization energy. This assumption holds well for $\mathrm{LaBr_3:Ce^{3+}}$, but significant deviations exist for NaI:Tl^+ because of its well known nonproportionality in the response.

Fig. 6 compares the $^{24}\mathrm{Na}$ spectra for both scintillators; that of $\mathrm{LaBr_3:Ce^{3+}}$ is the same as in Fig. 5. We made the spectra to coincide at 2.75 MeV. One first notices that the energy resolution of the total absorption peaks (1) and (9) and the double 511 keV escape peak (7) is much better in the case of $\mathrm{LaBr_3:Ce^{3+}}$. Note that the double 511 keV escape peaks (7) in both spectra are at the same position, but the 1.38 MeV total absorption peak (9) and the 511 keV backscatter peak (13) are shifted slightly to the right for NaI:Tl^+. This is a manifestation of the nonproportional response of NaI:Tl^+. For the same reason the single 511 keV escape peak (5) is shifted slightly to the right for NaI:Tl^+. Such shift was recently simulated by Monte Carlo techniques [10]. The total attenuation coefficient at 511 keV in NaI is 35% smaller than that of $\mathrm{LaBr_3}$ leading to slightly larger 511 keV escape probability. The effect is not very large because the intensity ratio between the escape peaks (7) and (5) is about the same for both scintillators.

To test the scintillators at high gamma ray energies, the spectrum of the $^{238}\mathrm{Pu}(^{13}\mathrm{C})$ source was measured, see Fig. 7. It shows a very rich line spectrum. Some peaks originate from the background. For example the line at 662 keV is from a too nearby $^{137}\mathrm{Cs}$ source. The origin of the peak near 1450 keV can be twofold. It may arise from 1461 keV gamma rays from $^{40}\mathrm{K}$ in surrounding construction material. It may also arise from the 1436 keV gamma peak from the decay of $^{138}\mathrm{La}$ isotopes. The same line together with lines from intrinsic α-activity was observed in $\mathrm{LaCl_3:Ce}$. [5] We do not exclude that intrinsic α activity in the $\mathrm{LaBr_3:Ce}$ scintillator contributes to the background spectrum between 1600 and 2700 keV in Fig. 7(b).

The high energy part of the spectrum is shown on a linear scale in Fig. 8. It shows the total absorption peak at 6129 keV together with the single 511 keV escape at 5618 keV and the double 511 keV escape peak at 5107 keV. The ratio between the intensity of the double and single 511 keV escape peaks for $\mathrm{LaBr_3:Ce^{3+}}$ and NaI:Tl^+ is similar as in Fig. 6. The small misalignments between the peak positions of both scintillators are again caused by nonproportional response.

Fig. 9 compares the pulse height spectra of the $^{60}\mathrm{Co}$ source. The energy resolution at 1.17 MeV (2) and 1.33 MeV (1) are much better for the $\mathrm{LaBr_3:Ce^{3+}}$ scintillator. Note that the two peaks are completely separated, and the only counts found in between both peaks are from multiple Compton scattering events.

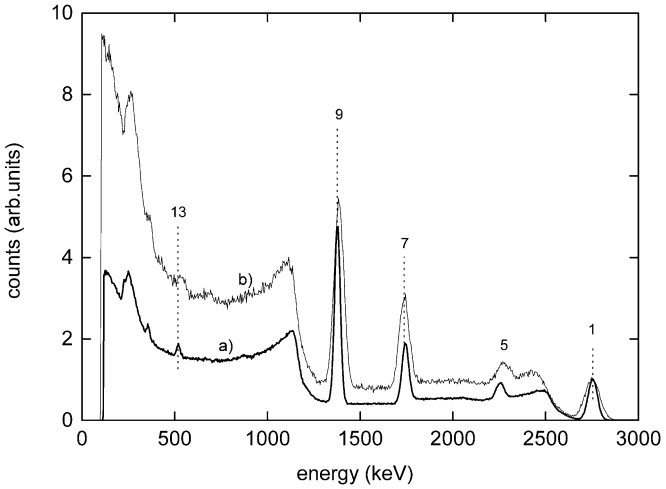

Fig. 6. The pulse height spectrum of $^{24}\mathrm{Na}$ measured with: a) the $\mathrm{LaBr_3:Ce^{3+}}$ and b) the NaI:Tl^+ scintillator.

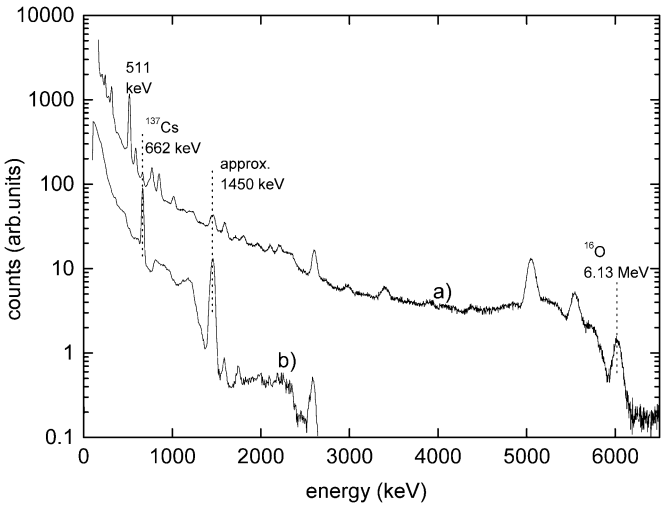

Fig. 7. a) The pulse height spectrum of the $^{238}\mathrm{Pu}(^{13}\mathrm{C})$ gamma source measured with the $\mathrm{LaBr_3:Ce^{3+}}$ scintillator. b) The background detected with $\mathrm{LaBr_3:Ce^{3+}}$.

The energy $E_C(1330) = 1120\,\mathrm{keV}$ and $E_C(1170) = 960\,\mathrm{keV}$ of the start of the Compton edges are indicated at (3) and (4), (5) is the double 511 keV escape peak at 310, and (6) the Compton backscatter peak with a maximum at 234 keV. The peaks for NaI:Tl do not align because of nonproportionality. Features (7) and (8) are detections of gamma rays that underwent two times or three times Compton scattering in the surrounding material.

The spectra for the $^{137}\mathrm{Cs}$ source are shown in Fig. 10. The energy resolution in the 661.6 keV total absorption (1) peak is 3.4% for $\mathrm{LaBr_3:Ce^{3+}}$ and 6.4% for NaI:Tl^+. The Compton edge (2) at 477 keV, the single (3) and double (4) backscatter peak and the peak from Ba K_α X-rays (5) can be seen.

The $^{133}\mathrm{Ba}$ spectra are shown in Fig. 11. The peaks numbered 1–9 are the gamma ray lines at 383.9, 356.0, 302.9, 276.4, 223.1, 160.6, 81.0, 79.6, and 53.2 keV from the source. The peaks numbered 5 and 6 are too weak and disappear in the Compton background. In the spectrum measured with NaI:Tl one also observes the Cs K_α X-ray line at 31.0 keV. Note, that the resolution with $\mathrm{LaBr_3:Ce^{3+}}$ at energies around 300 keV is better than with NaI:Tl and peaks 1 and 2 are clearly resolved.

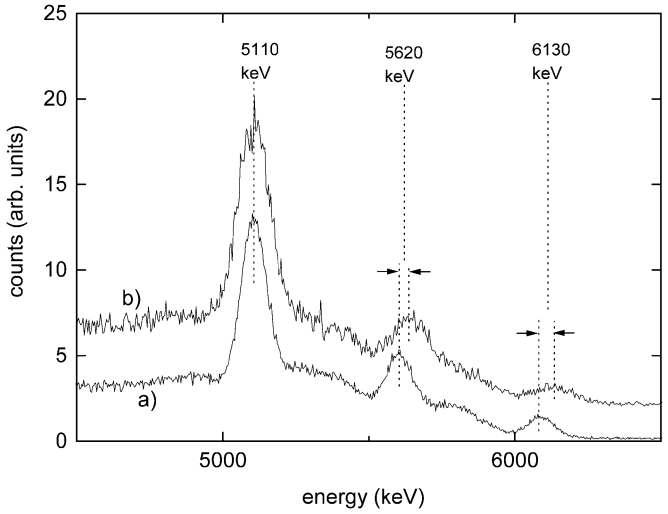

Fig. 8. High energy part of the pulse height spectra of the $^{238}Pu(^{13}C)$ gamma source measure by: a) $LaBr_3:Ce^{3+}$. b) Spectrum measured by NaI:Tl is offset by two units.

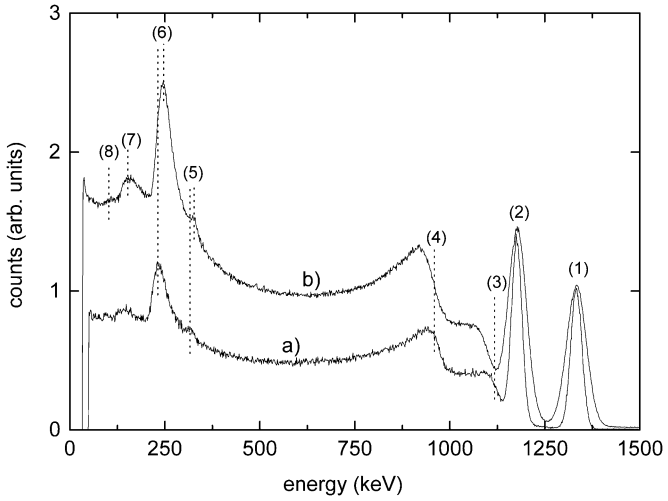

Fig. 9. Pulse height spectra of the ^{60}Co source with: a) $LaBr_3:Ce^{3+}$ and b) NaI:Tl.

The ^{241}Am spectra are shown in Fig. 12. The Compton backscatter peak of 59.5 keV gamma rays is observed above the threshold at 48.3 keV (2). The total attenuation coefficient at 59.5 keV is $\approx 25\ \mathrm{cm}^{-1}$ for both scintillators and most of the 59.5 keV gamma rays are absorbed within 1 mm below the surface of the crystal. The small penetration depth allows the escape of characteristic X-rays from La, I, or Br. (3) and (4) are caused by 28.3 and 28.6 keV K_α and 32.2 and 32.3 keV K_β Iodide X-ray escape from NaI. (5) is from the escape of 33.0 and 33.4 keV La K_α X-rays. At 21.8 keV the escape peak of 37.7 and 37.8 keV K_β La X-rays is expected, but it overlaps with detection of Np X-rays between 16 and 22 keV (6) from the ^{241}Am source. Escape of 11.9 keV Br K_α gives a contribution (7) around 47.6 keV. Whereas in all previous spectra the energy resolution of the total absorption peak is always better with $LaBr_3:Ce^{3+}$ than with NaI:Tl^+, the situation is reversed for detection of 59.5 keV gamma rays where NaI:Tl^+ shows better energy resolution.

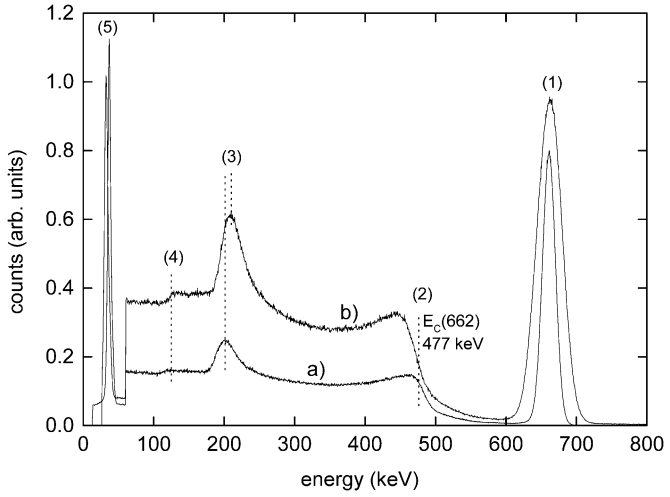

Fig. 10. Pulse height spectra of the ^{137}Cs source with: a) $LaBr_3:Ce^{3+}$ and b) NaI:Tl. The part up to 60 KeV is shown on a two times and five times smaller scale for a) and b) respectively.

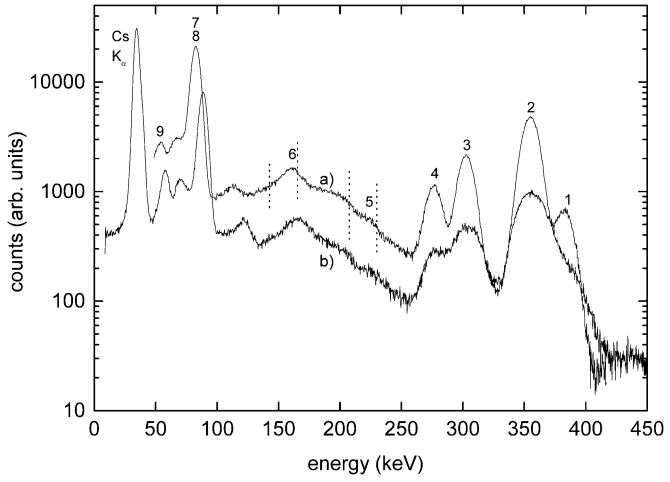

Fig. 11. Pulse height spectra of the ^{133}Ba source with: a) $LaBr_3:Ce^{3+}$ and b) NaI:Tl.

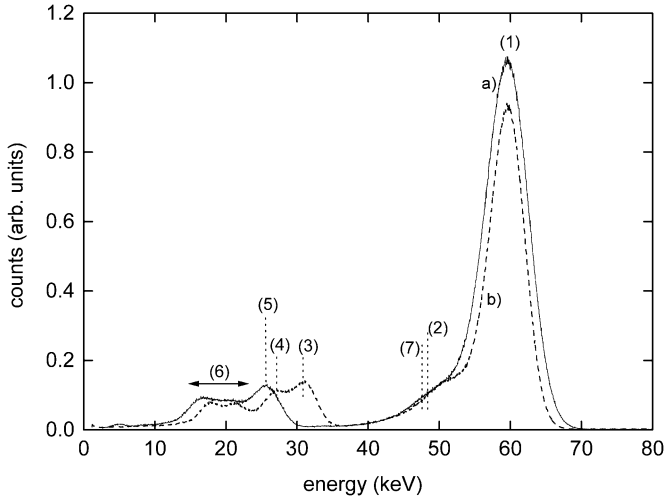

Fig. 12. Pulse height spectra of the ^{241}Am source with a) solid curve $LaBr_3:Ce^{3+}$ and b) dashed curve NaI:Tl.

As a final example the spectrum of the Tb target of the variable X-ray source is shown in Fig. 13. With the NaI:Tl scintil-

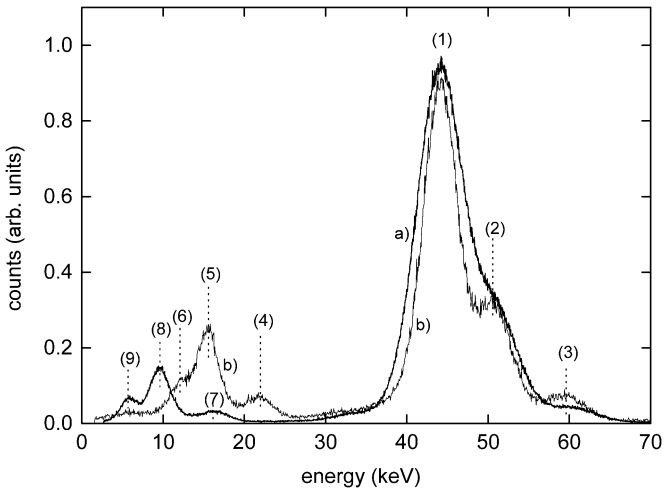

Fig. 13. Pulse height spectra from the Tb target in the variable X-ray source with: a) $LaBr_3 : Ce^{3+}$ and b) NaI:Tl.

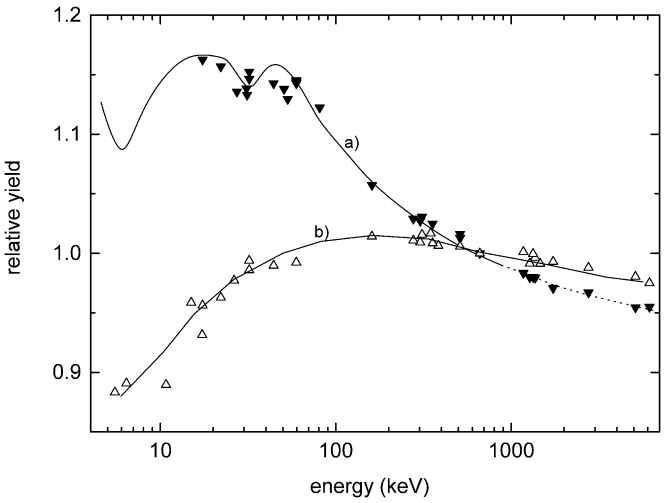

Fig. 14. The proportionality curve for: a) NaI:Tl (solid symbols), and b) $LaBr_3 : Ce^{3+}$ (open symbols). The solid curve through the NaI:Tl data is from Aitken *et al.* [14]. The dashed curve is an extension toward 6 MeV from our work. Above 100 keV the errors are of the same magnitude as the symbol size. Errors increase to ± 0.02 at energies around 10 keV.

lator the peaks from detection of K_α (1) and K_β (2) X-rays from Tb at 44.2 and 50.7 keV are resolved in the spectrum. For the $LaBr_3$ scintillator the resolution is worse and the two peaks are not resolved. (3) is the detection of ^{241}Am 59.5 keV gamma rays. (4) and (5) are Iodide K_α escape peaks and (6) is an Iodide K_β escape peak. (7), (8), and (9) is the same sequence of escape peaks but then for La in $LaBr_3 : Ce^{3+}$.

D. Light Yield and Non-Proportional Response

When the pulse height spectra measured with $LaBr_3$ were compared with those measured with NaI we already noticed the nonlinearity between pulse height and detected gamma ray energy. It is well established that this nonlinearity is due to a nonlinearity in the scintillator photon yield with the energy of the primary electron [11]. Therefore, ideally the response to electrons should be determined as can be done by means of the Compton Coincidence Scattering Technique [12].

The absolute photoelectron yield was determined for the gamma ray spectra measured at $V_c > 500$ V by comparison with the single photoelectron spectrum. At lower cathode voltage, the single photoelectron spectrum disappears in the noise of the amplifiers because of too low PMT gain, and the method does not work anymore. In those cases the absolute yield was determined by comparing the pulse height at low voltage with the pulse height at the same energy measured at higher voltage. For example the 511 keV line in Fig. 7 measured at $V_c = -300$ V is also present in the spectrum of the ^{24}Na, the ^{60}Co, and the ^{22}Na source. The 511 keV peak can also be measured at higher V_c. By cross relating the different spectra each spectrum can be calibrated. Occasionally the peak of interest was fitted by a Gaussian shaped curve to resolve it better from other partly overlapping peaks.

The absolute scintillator yield for $LaBr_3 : Ce^{3+}$ at 662 keV and 0.5 μs and 10 μs shaping time is 13 000 phe/MeV and 14 000 phe/MeV. This is somewhat smaller than the yield of 14 450 phe/MeV found for the NaI:Tl scintillator at 3 μs shaping. It is also slightly smaller than 14 800 phe/MeV that we reported before for a $3 \times 3 \times 10$ mm^3 $LaBr_3 : 0.5\%Ce^{3+}$ sample in a quartz ampoule [2]. The yield as function of gamma or X-ray energy relative to the yield at 662 keV is shown in Fig. 14.

The light yield of $LaBr_3 : Ce^{3+}$ in Fig. 14 shows a very good (1.00 ± 0.02) proportionality at energies between 30 keV and 6 MeV. There is a tending decrease in efficiency by a few percent at energies from 200 keV to 6 MeV. On the low energy side from 30 to 6 keV the yield drops by $\approx 10\%$. This behavior is quantitatively similar to the electron response curve that we measured for a $LaCl_3 : Ce^{3+}$ scintillator [13].

The response curve for NaI:Tl shows a different behavior than $LaBr_3 : Ce^{3+}$. In Fig. 14 results by Aitken *et al.* [14] reported already in 1967 and confirmed many times since are included. Our data provide an extension toward 6 MeV but for the rest agree with literature. From 6 MeV down to 30 keV the relative yield continuously increases by as much as 20%. Between 60 keV and 10 keV the response is relatively constant apart from a dip at the iodine K-shell absorption edge [14]–[16].

When we assume optimal PMT properties, i.e., a high quantum efficiency of 30%, a light collection efficiency of 100%, and a photoelectron efficiency of 100%, we obtain for NaI:Tl a photon yield of at least 48 000 photons/MeV at 662 keV and 56 000 ph/MeV at 50 keV. Similar values were reported by Balcerzyk *et al.* [5] These numbers are much larger than the always advertised value of 40 000 ph/MeV.

E. Energy Resolution

The energy resolution can be written as [11]

$$R^2 = R_{\text{stat}}^2 + R_{\text{np}}^2 + R_{\text{inh}}^2 + R_{\text{det}}^2 \tag{2}$$

where R_{stat} is the contribution from the statistics in the number N_{phe} of photoelectrons. R_{np} is a contribution connected with nonproportionality in the scintillation light yield with gamma ray or electron energy. R_{inh} is a contribution from in-homogeneities or nonuniformities in the scintillator, the light reflector or the quantum efficiency of the photon detector. R_{det} is a contribution from noise and variance in the gain of the photon detector.

The last two contributions are related to crystal growth and detector technology. The first two are fundamental in nature and intrinsic to the scintillator.

When we assume that the number of detected photons follows Poisson statistics then one may write

$$R^2 = 5.55\frac{1+v(M)}{N_{\mathrm{phe}}} + R_{\mathrm{np}}^2 + R_{\mathrm{inh}}^2. \tag{3}$$

The resolution is defined here as the full width at half maximum (FWHM) divided by the energy. R_{det} is incorporated into $v(M)$ which is the variance in the photomultiplier gain. Its value can be obtained from the width of the single photoelectron spectrum [11]. We determined $v(M)$ for the PMT used in this work. When operating it at $V_c = -900\,\mathrm{V}$, $v(M) = 0.07$, but at lower voltage, the width of the single electron spectrum increases because the number of secondary electrons emitted from the first dynode decreases. $v(M) = 0.09$ at $-700\,\mathrm{V}$ and 0.15 at $-500\,\mathrm{V}$. Because of too low gain we could not measure the single electron spectrum at $-300\,\mathrm{V}$, but we estimate a value between 0.20 and 0.30. It should be remarked that R_{inh} may depend on N_{phe}.

The energy resolution R was determined from the peaks in the pulse height spectra. Isolated peaks were always fitted with a single Gaussian function, but occasionally the peaks were fitted with two Gaussian functions in order to better separate the peak of interest from other partly overlapping peaks. The results are shown in Fig. 15.

The data for $LaBr_3:Ce^{3+}$ between 40 keV and 2 MeV display an energy resolution that decreases with the square root of the gamma ray energy. At 662 keV the resolution is 3.4%. In the past we reported for a crystal of $3 \times 3 \times 10\ \mathrm{mm}^3$ dimension a resolution of $2.8 \pm 0.2\%$ [2]. Reanalysis of the old data on the small crystal by fitting with a single Gaussian shaped function over the same interval of energy as used for the large crystal now reveals a resolution of $3.2 \pm 0.2\%$. It demonstrates that the upgrade from the small sample to a large commercial sized scintillator does not lead to much deterioration of scintillator performance. The resolution levels off to a value around 1.8% for energies beyond 2 MeV, which signals other contributions to the energy resolution than statistics in the number of photoelectrons alone. Since the proportionality of the scintillator is good at high energies, a large contribution from R_{np} is not expected and the main contribution then comes from R_{inh}. The solid curve through the data is the resolution calculated with (3) using the experimental values for N_{phe} and $R_{\mathrm{inh}} = 1.6\%$ together with an estimated value of $v(M) = 0.25$.

At energies below 40 keV the resolution significantly degrades as compared to the resolution calculated from photon statistics. Note that at the same energies the scintillator starts to show nonproportional behavior (see Fig. 14), suggesting a relationship. Another reason may be the fact that these low energy X-rays are absorbed close to the surface of the scintillator, the energy resolution then becomes quite sensitive to variations in surface properties and reflection coefficients leading to larger R_{inh}. If so, we may expect improvements when better packaging techniques for $LaBr_3:Ce^{3+}$ scintillators are developed.

Fig. 15 shows also the energy resolution found with the NaI:Tl scintillator. Similar results can be found in [5], [17]. The resolution at 662 keV is 6.4% which is normal for good quality $NaI:Tl^+$ scintillators. However, despite a larger photoelectron yield, it is almost two times worse than the resolution of 3.4% observed for $LaBr_3:Ce^{3+}$. The reason is the very large contribution from R_{np}. At energies below 100 keV the situation improves much for NaI:Tl whereas the situation for $LaBr_3:Ce^{3+}$ becomes less advantageous. The photoelectron yield of NaI:Tl around 50 keV is 17 000 phe/MeV which is significantly larger than for $LaBr_3:Ce^{3+}$. Also between 10 and 100 keV the response of NaI:Tl is relatively proportional with energy (see Fig. 14). This together with possibly more homogenous surface properties and reflectivity in the NaI:Tl scintillator are probably the main reasons for the better energy resolution below 100 keV.

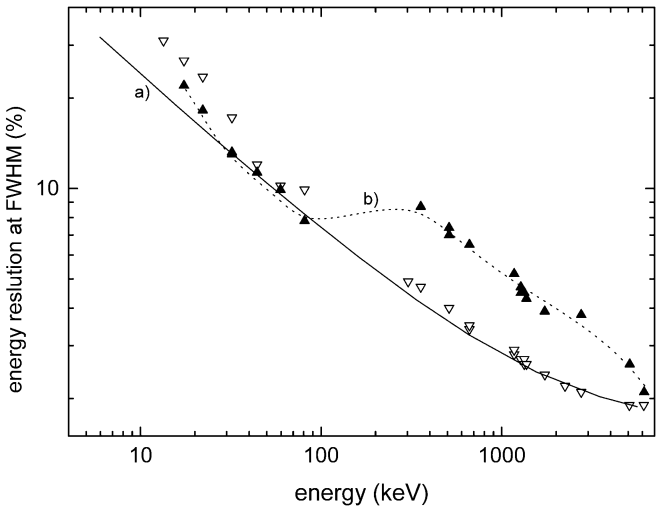

Fig. 15. The energy resolution measured with (open symbols) $LaBr_3:Ce^{3+}$ and (solid symbols) $NaI:Tl^+$; solid curve a) is calculated from (3) and dashed curve b) is drawn to guide the eye.

IV. Summary and Conclusion

In this work, the scintillation properties of a commercially grown $\varnothing 19 \times 19\,\mathrm{mm}^3$ $LaBr_3$ scintillator were studied. The results demonstrate that the scaling up from a laboratory sized crystal of small dimension ($0.09\ \mathrm{cm}^3$) to a crystal of $6\ \mathrm{cm}^3$ volume does not lead to much deterioration of the scintillation properties. The total light yield is slightly smaller than what we found on the small crystal in the past, and the FWHM energy resolution at 662 keV is 3.4% in stead of 3.2% for the small crystal. The laboratory studies in the past were performed on a sample contained in a quartz ampoule surrounded by reflecting Teflon tape [2]. In the commercial scintillator, the crystal is sealed in an aluminum container covered with reflecting material and sealed off with a glass window. We conclude that the technology is at such level that the scintillation properties are maintained very well.

Because of the high potential that $LaBr_3:Ce^{3+}$ scintillators will be used for gamma ray spectroscopy purposes, pulse height spectra of a variety of gamma and X-ray sources were made and compared with those of the most commonly used scintillator $NaI:Tl^+$. The $LaBr_3:Ce^{3+}$ spectra demonstrate a much better proportionality between pulse height and gamma ray energy. Furthermore, energy resolution at energies above 100 keV are much (almost a factor of two) better than with $NaI:Tl^+$.

For gamma ray spectroscopy these are very advantageous properties. More work needs to be done, to improve the energy resolution below 100 keV where NaI:Tl performs better. In this work we used the Hamamatsu R1791 PMT that does not cope well with the high peak currents caused by the fast and intense scintillation pulses from $LaBr_3 : Ce$. A linear focused PMT with a box and grid dynode as a first stage would have been a better choice. We anticipate that with $v(M) \approx 0.07$ the energy resolution around 1 MeV can be improved by about 0.2%.

The photoelectric attenuation coefficient of $LaBr_3$ is very similar to that of NaI:Tl, but the Compton scattering coefficient in $LaBr_3$ is about 40% larger, and the pair creation coefficient is 25% larger. Compton scattering followed by photoelectric absorption of the scattered gamma ray are the events that provide the most important contribution to the full energy peak at energies around and above 1 MeV. This means that when large sized (5–8 cm diameter) $LaBr_3 : Ce$ crystals are used, the count rate in the full energy peak will be significantly larger than with a NaI:Tl scintillator of the same dimensions.

The eight times faster decay of the scintillation pulse makes $LaBr_3 : 0.5\%Ce^{3+}$ also very useful in high count rate and/or fast timing resolution experiments. This aspect is even further improved when the concentration of Ce^{3+} is increased to above 2%. In that case, the scintillation decay decreases from 30 to 15 ns (see Fig. 4) and the timing resolution also improves significantly [8].

ACKNOWLEDGMENT

The authors would like to thank the company Saint Gobain, Division of Crystals and Detectors, Nemours, France, for providing the $\varnothing 19 \times 19\ mm^3$ $LaBr_3 : Ce^{3+}$ and NaI:Tl^+ scintillators used in this work.

REFERENCES

[1] P. Dorenbos, C. W. E. van Eijk, H. U. Güdel, K. W. Krämer, and E. V. D. van Loef, "Scintillator Crystals, Method for Making Same, Use Thereof," Int. Patent WO 01/6945 A2, Feb. 16, 2001.

[2] E. V. D. van Loef, P. Dorenbos, C. W. E. van Eijk, K. Krämer, and H. U. Güdel, "High-energy-resolution scintillator: Ce^{3+} activated $LaBr_3$," *Appl. Phys. Lett.*, vol. 79, pp. 1573–1575, 2001.

[3] E. V. D. van Loef, "Scintillation properties of $LaBr_3 : Ce^{3+}$ crystals: Fast, efficient and high-energy-resolution scintillators," *Nucl. Instrum. Methods*, vol. A486, pp. 254–258, 2002.

[4] E. V. D. van Loef, P. Dorenbos, C. W. E. van Eijk, K. Krämer, and H. U. Güdel, "High-energy-resolution scintillator: Ce^{3+} activated lacl $_3$," *Appl. Phys. Lett.*, vol. 77, pp. 1467–1468, 2000.

[5] M. Balcerzyk, M. Moszynski, and M. Kapusta, "Comparison of $LaCl_3 : Ce$ and NaI(Tl) scintillators in γ-ray spectrometry," Nucl. Instrum. Methods, 2004, to be published.

[6] K. S. Shah, J. Glodo, M. Klugerman, W. W. Moses, S. E. Derenzo, and M. J. Weber, "$LaBr_3 : Ce$ scintillators for gamma ray spectroscopy," presented at the IEEE Conference on Nuclear Science, Norfolk, VA, 2002. Presentation N8-2.

[7] W. W. Moses, "Time of flight in PET revisited," *IEEE Trans. Nucl. Sci.*, vol. 50, pp. 1325–1330, Oct. 2003.

[8] A. Kuhn, S. Surti, J. S. Karp, P. S. Raby, K. S. Shah, A. E. Perkins, and G. Muehllehner, "Design of a lanthanum bromide detector for TOF PET," *IEEE Trans. Nucl. Sci.*, submitted for publication.

[9] P. Dorenbos, J. T. M. de Haas, R. Visser, C. W. E. van Eijk, and R. W. Hollander, "Absolute light yield measurements on BAF_2 crystals and the quantum efficiency of several photomultiplier tubes," *IEEE Trans. Nucl. Sci.*, vol. 40, pp. 424–430, Aug. 1993.

[10] R. P. Gardner and A. Sood, "A monte carlo simulation approach for generating nai detector response functions (DRF's) that accounts for nonlinearity and variable flat continua," *Nucl. Instrum. Methods*, vol. B213, pp. 87–99, 2004.

[11] P. Dorenbos, J. T. M. de Haas, and C. W. E. van Eijk, "Non-proportionality in the scintillation response and the energy resolution obtainable with scintillation crystals," *IEEE Trans. Nucl. Sci.*, vol. 42, pp. 2190–2202, Oct. 1995.

[12] J. D. Valentine and B. D. Rooney, "Design of a compton spectrometer experiment for studying scintillator nonlinearity and intrinsic energy resolution," *Nucl. Instrum. Methods*, vol. A353, pp. 37–40, 1994.

[13] E. V. D. van Loef, W. Mengesha, J. D. Valentine, P. Dorenbos, and C. W. E. van Eijk, "Non-proportionality and energy resolution of a $LaCl_3 : 10\%Ce^{3+}$ scintillation crystal," *IEEE Trans. Nucl. Sci.*, vol. 50, pp. 155–158, Feb. 2003.

[14] D. W. Aitken, B. L. Beron, G. Yenicay, and H. R. Zulliger, "The fluorescent response of NaI(Tl), CsI(Tl), CsI(Na), and CaF_2 (Eu) to X-rays and low energy gamma rays," *IEEE Trans. Nucl. Sci.*, vol. NS-14, pp. 468–468, Aug. 1967.

[15] L. R. Wayne, W. A. Heindl, P. L. Hink, and R. E. Rothschild, "Response of NaI(Tl) to X-rays and electrons," *Nucl. Instrum. Methods*, vol. A411, pp. 351–364, 1998.

[16] L. F. Requicha Ferreira, H. M. N. B. L. Ferreira, J. F. C. A. Veloso, and J. M. F. D. Santos, "Energy nonlinearity effects in the response of ionic crystal scintillators to X-rays with energy in the region of the K-absorptions edges: Experimental results," *Nucl. Instrum. Methods*, vol. A516, pp. 486–491, 2003.

[17] M. Moszynski, J. Zalipska, M. Balcerzyk, M. Kapusta, W. Mengesha, and J. D. Valentine, "Intrinsic energy resolution of NaI(Tl)," *Nucl. Instrum. Methods*, vol. A484, pp. 259–269, 2002.